

Chapter 3: Modeling of Absorbed Power Coupling Efficiency

In this chapter, the modeling of absorbed power coupling efficiency is introduced. The amount of absorbed power on the device can be adjusted by modulating the power of incoming optical signal, and this modulation results in a device with wavelength dependence.

3.1 Impedance matching thin-film absorber with mirror

Microbolometer design can be separated into two parts. The first part is optimizing the sensing of resultant temperature, and the other part is the absorption of radiation. In an ideal device, the absorber must provide total absorption of the incoming radiation and furthermore, it must convert the electromagnetic radiation into heat. This chapter focuses on the design of a structure with an absorbed power coupling efficiency that is wavelength dependent.

Broadband absorption of a thin conducting film can be obtained using impedance matching techniques [1]. As absorption of IR radiation in the thin metal is due to free charge carrier [2], the absorption properties of the metal layer can be determined from the conductivity of thin film absorber. If a wave impinges at normal incidence on a thin sheet of a material in air, as shown in Fig.3.1, the sheet resistance is

$$R_{sheet} = \frac{1}{\sigma \cdot h}, \quad (3.1)$$

where h is the thickness and σ is the conductivity of the thin absorber..

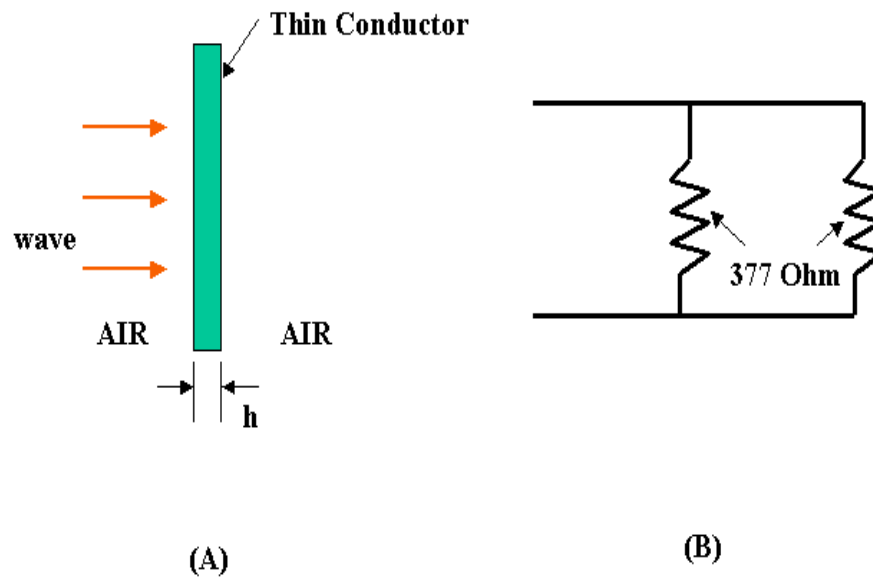


Figure 3.1 Schematic view of matching a radiation absorber to free space; (A). Geometry (B) Equivalent Circuit.

Broadband absorption of a thin conducting film is obtained when this sheet resistance is matched to the impedance of free space (377 ohm) [1]. The required conductivity is

$$\mathbf{s} = \frac{1}{377 \cdot h} \quad (\text{ohm-cm})^{-1} \quad (3.2)$$

As long as the required conductivity of absorbing material remains unchanged within the operating wavelength region, the impedance matching technique is a valid approach for broadband absorption. The amount of power absorbed, transmitted, and reflected is calculated as 4/9, 4/9, and 1/9 of the incoming incident power, respectively. Thus 44 percent of the incident power is absorbed without explicit wavelength dependence.

It is important to understand when performing the calculations the key difference between circuit theory and transmission line theory. Circuit analysis assumes that the physical dimensions of a network are much smaller than the electrical wavelength, while transmission lines may be a considerable fraction of a wavelength, or many wavelengths, in size. Thus a transmission line is a distributed parameter network, where voltage and current can vary in magnitude and phase over its length. Due to the range of wavelength involved here, the entire equivalent circuit has to be treated as a distributed network of transmission lines [3].

Enhanced absorption can be increased by placing a reflecting short at one-quarter wavelength behind the absorbing layer, but would make the absorber wavelength sensitive. Figure 3.2 shows the modified configuration of matching impedance to free space shown in figure 3.1. Theoretically, over 90% enhanced radiation absorption in a thin film can be achieved at the resonant point with a perfect mirror placed $[(\text{odd integer})/4] \cdot \lambda$ behind the absorbing layer. The mirror

layer must be a perfect mirror, i.e., must use a material with a high conductivity. For example, gold is a good candidate as a mirror material due to high conductivity and high reflectivity at infrared wavelengths [4].

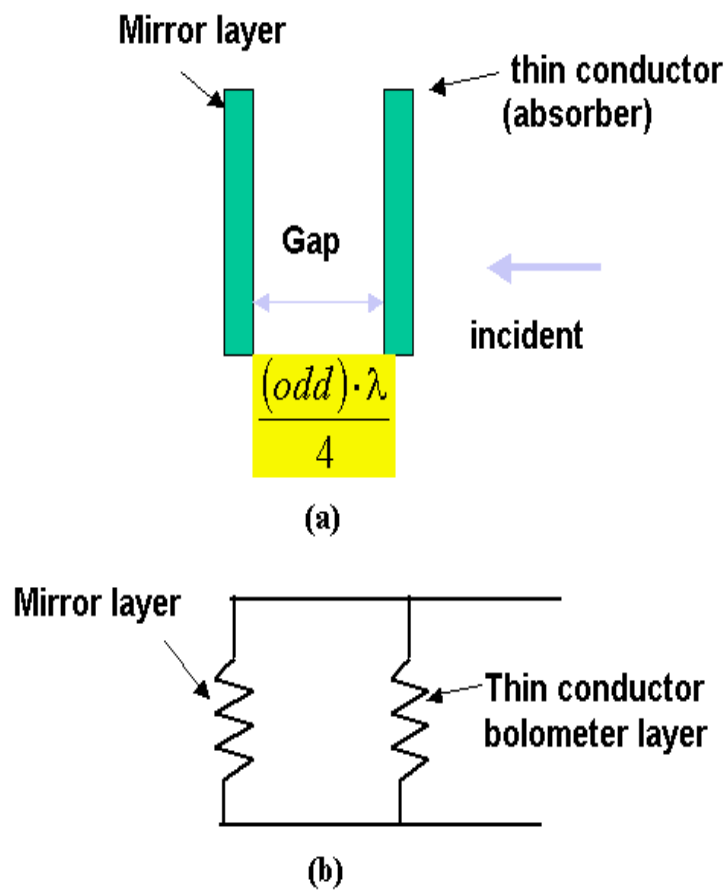


Figure 3.2 Schematic view of enhanced radiation absorption in a thin film with mirror placed $[(\text{odd integer})/4] \cdot \lambda$ behind absorbing layer. (a) Geometry and (b) Equivalent circuit.

Assuming that the power spectral density is constant, the power coupling spectral response for different air gaps is shown on figure 3.3. The numeral 1 on the y-axis indicates 100% absorption of all the incoming power at a specific wavelength. If the air gap between the absorber and the mirror layer is 1.5 μm , the first resonance is generated at 6 μm . The second and third resonances are generated at 2 μm and 1.2 μm , respectively.

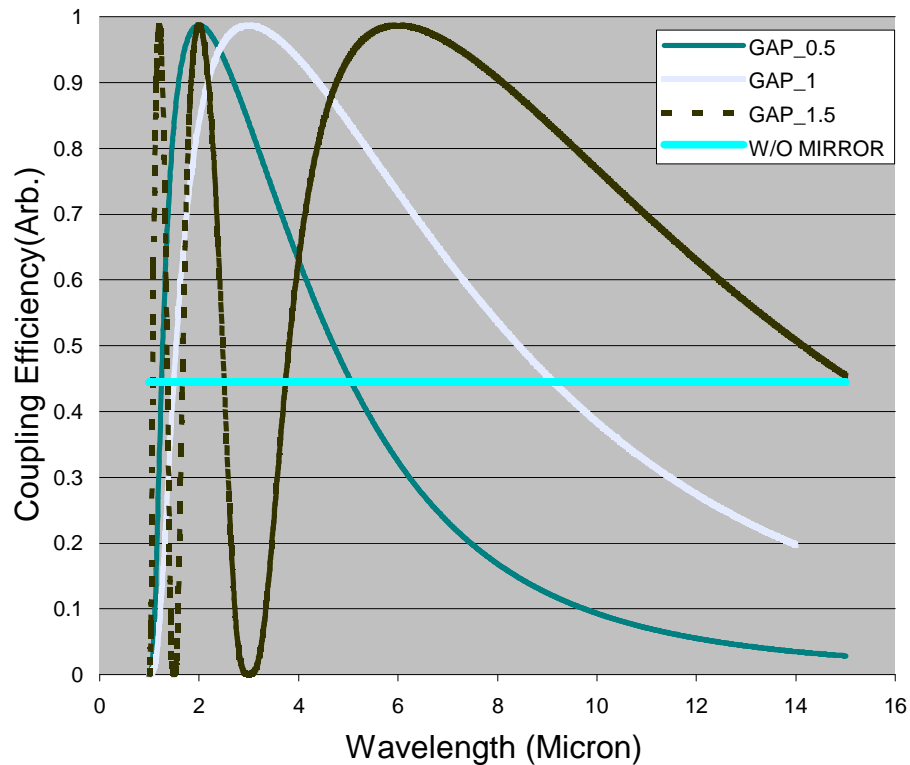


Figure 3.3 Simulation result of coupling efficiency ($P_{\text{absorbed}}/P_{\text{incident}}$) with matching impedance at free space (377 ohms), placing a reflecting short at one-quarter wavelength behind thin conductor.

3.2 Model of absorbed power coupling efficiency

In the real world, the bolometer layer structure and mirror coating structure cannot exist as shown in figure 3.2. Several dielectric layers and a sacrificial layer are deposited and etched to construct the microbolometer structure. Due to the dielectric supporting structure, a microbolometer without a mirror will not generate the same flat broadband response such as shown in figure 3.3. The dielectric layers supporting the bolometer layer work together as a weak mirror. Since it is not a perfect mirror it does not generate the peak resonance produced by perfect mirror.

For this wavelength selective microbolometer, several considerations are imposed on microbolometer design, as follows: Firstly, every process should be IC compatible for silicon monolithic devices. Therefore, silicon nitride and silicon oxide are reasonably good materials to choose as dielectric layers. The thickness of each layer should not exceed several microns (1-2 μm) in terms of IC fabrication compatibility.

Secondly, the thickness of the multi-stack membrane should be chosen to insure that the structure of the microbolometer is mechanically stable as well. This can be achieved by combining the tensile nature of silicon nitride and the compressive nature of silicon dioxide [5][6][7]. Total residual stress of the stack should be weak tensile stress to allow the membrane to remain flat after completion of the stress sensitive microbolometer. Han experimentally determined that the ratio of the silicon dioxide thickness to the silicon nitride thickness is optimized at about 3 to 3.5 [8]. With the ratio of 3 to 3.5, the residual

stress of the composite membrane is 0.1 to 0.3 GPA. This can be measured using the beam curvature method. At the ratio of 2, the excessive tensile stress may cause multi stack films to crack. At the ratio of 5, excessive compressive stress may cause buckling. Experimentally, total thickness of the membrane structure should be over 5000 Å in order to survive the sacrificial releasing process.

Therefore, when designing the thickness of each layer, thickness of films should be chosen for the spectral response with consideration of the physical limitations imposed by mechanical stability. The microbolometer structure can be modeled as the following equivalent circuit, governed by transmission line equations, as shown in figure 3.4.

The actual structure that matches with the model is shown in figure 3.5. Selection of relative dielectric constant, thickness, and number of dielectric layers are determined by targeting wavelength selectivity. In the transmission line equation, the thickness and relative dielectric constant (ϵ_r) of each layer are considered in order to calculate the absorbed power at the bolometer layer. The q_k layer shown in figure 3.5 can be the air gap or a dielectric depending on configuration of fabrication.

In the transmission line equivalent model, the wave impedance and the propagation constant of each layer have to be determined by calculating the input and the load impedance of the each layer. The wave impedance of the incoming infrared wave passing through each layer q , defined as the ratio of the \overline{E} and \overline{H} fields can be represented as Eqn 3.3. In a lossless medium of dielectric material layers, ϵ and μ are real numbers.

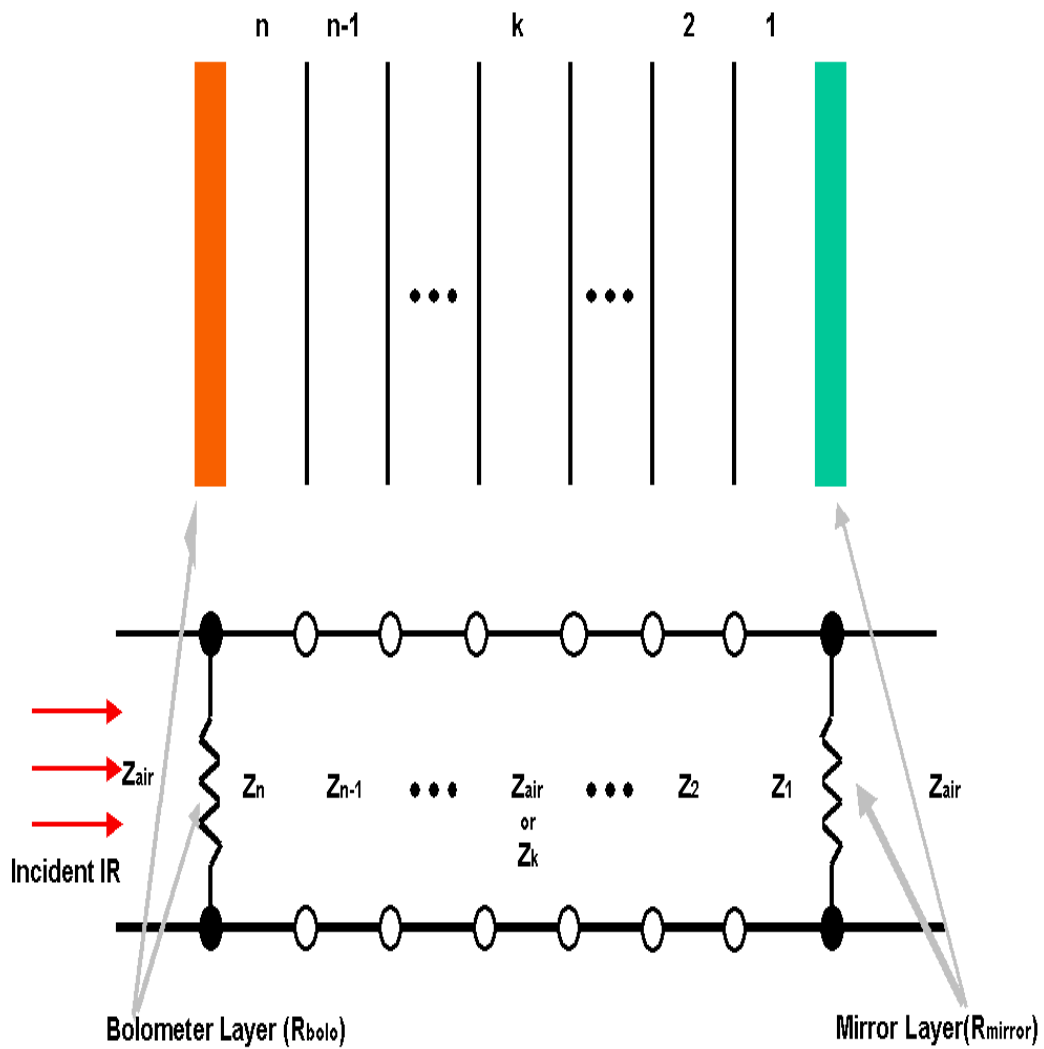


Figure 3.4 Schematic diagram of transmission line equivalent circuit model of multi stack micromachined structure with bolometer layer and mirror coating layer.

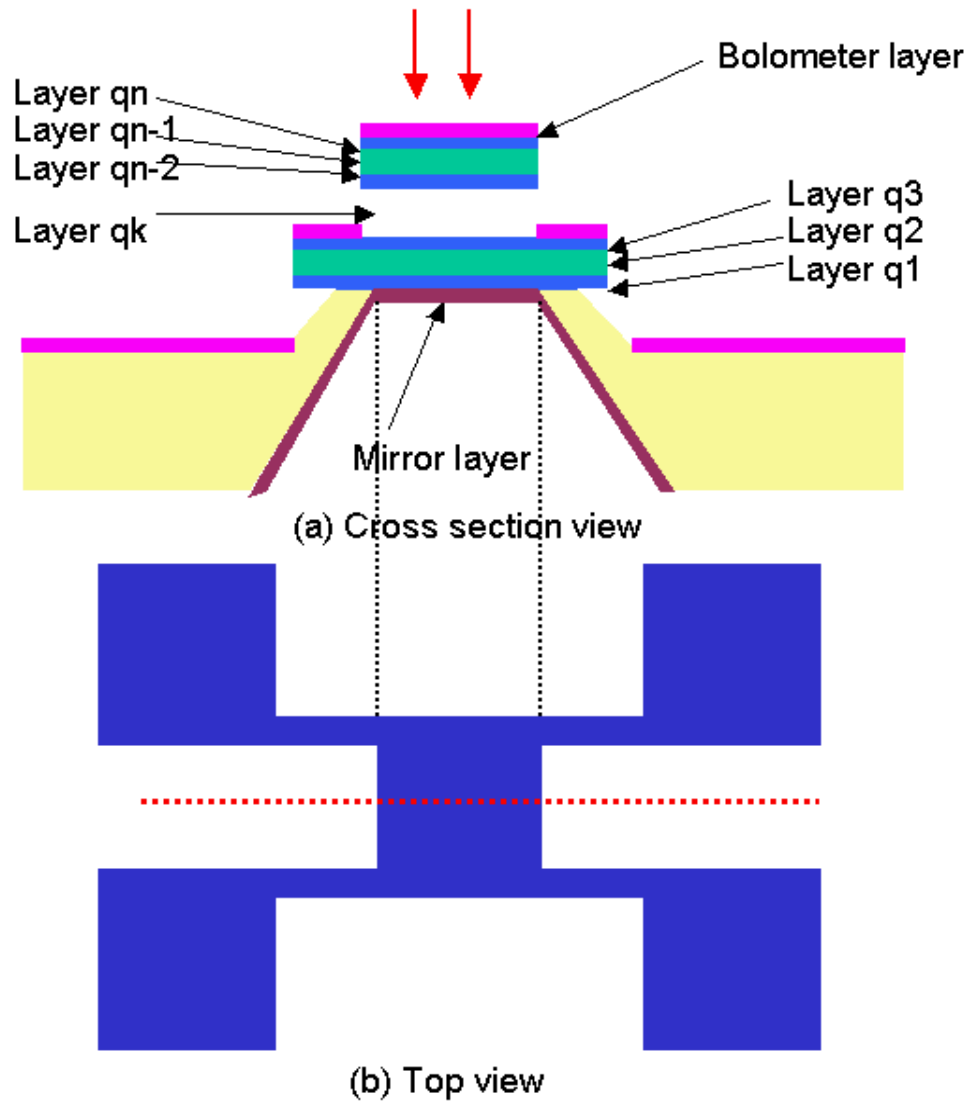


Figure 3.5 Actual structure with cross sectional view, matching with transmission model shown in Fig.3.4.

The wave impedance of passing through each layer q is

$$\mathbf{h} = \sqrt{\frac{\mathbf{m}}{\mathbf{e}}} = \mathbf{h}_0 \sqrt{\frac{\mathbf{m}_r}{\mathbf{e}_r}} = 377 \cdot \frac{1}{\sqrt{\mathbf{e}_r}}, \quad (3.3)$$

where \mathbf{h}_0 is the wave impedance of air, and relative permeability μ_r is 1.

The propagation constant of each layer at a given wavelength (λ) is defined as

$$\mathbf{g} = \frac{i2\mathbf{p}}{\mathbf{l}} \cdot \sqrt{\mathbf{e}_r}. \quad (3.4)$$

For each layer q , the input impedance seen looking into the transmission line must vary with the thickness of layer. At a distance l from the load, the input impedance seen looking toward the load is

$$Z_{in} = Z_o \frac{Z_L + Z_o \tanh(\mathbf{g} \cdot l)}{Z_o + Z_L \tanh(\mathbf{g} \cdot l)}, \quad (3.5)$$

where Z_o is the characteristic impedance of the q_{th} layer, which is the ratio of voltage and current for a traveling wave. Z_{in} is the input impedance of each layer and this is used as Z_L in subsequent calculations. Z_L is the load of each layer.

Calculated input impedance is an important result because it provides the input impedance of a transmission line with arbitrary load impedance. For the right side of equivalent circuit figure 3.4, eqn.3.5 is applied consecutively to the left. The calculated input impedance can be used as the load impedance for input impedance calculation for the next layer, to the left. The wave impedance explained above can be used as the characteristic impedance for the transmitting dielectric.

Finally, amplitude of the reflected wave normalized to the amplitude of the incident wave is known as the reflection coefficient Γ . At the surface of bolometer layer Γ is

$$\Gamma = \frac{Z_{tot} - Z_o}{Z_{tot} + Z_o}, \quad (3.6)$$

where Z_{tot} is the total impedance of all the dielectric layers and the microbolometer absorber.

Using the relationship of $T=1+\Gamma$, where T is the transmission coefficient, the amount of transmitted power to the bolometer is calculated as follows:

$$h_{bolo} = 377 \frac{(\text{Re}(1 + \Gamma))^2}{Z_{bolo}} \quad (3.7)$$

where h_{bolo} is the power coupling efficiency of the bolometer layer, Z_{bolo} is the sheet resistance of the bolometer layer, and 377 ohm is normalized factor.

The coupling efficiency between the incident wave and the absorbed wave can be calculated with the transmission line model explained above. As an alternative way of calculating the spectral response of a multi-stack film, the characteristic impedance matrix method is useful, and the result from both methods should be identical [9]. For design purposes, the selection of desired wavelength can be achieved by knowing the effective air thickness associated with all the thin films deposited. The summation of square roots of the relative dielectric constant (ϵ_r) of each layer decides the effective air thickness between thin metal bolometer layer and mirror layer.

$$gap_{effective} = \sum_{q=1}^n (\sqrt{\epsilon_r_q} \cdot l_q) \quad (3.8)$$

where $gap_{effective}$ is the effective air thickness, ϵ_r_q is the relative dielectric constant of each q layer, and l_q is the thickness of each q layer.

If the gap is filled with an air cavity, the first resonance is generated at a wavelength of 4 times the actual thickness of the air gap. For materials that have a large dielectric constant such as silicon nitride and silicon oxide, the effective air thickness of dielectric films is larger than the actual thickness of dielectric films.

The coupling efficiency of infrared detector is a function of sheet resistance of the bolometer, thickness of the dielectric, relative dielectric constant, and incoming wavelength. The power coupling efficiency model can incorporate the complex dielectric constant, though for simplicity, a real dielectric constant is used for simulation since the loss in silicon nitride and silicon oxide is small at the wavelengths studied here, this is a reasonable approximation.

Figure 3.5 shows the result of the power coupling efficiency calculation for the different micromachined wavelength selective structures. Table 3.1 shows that the dielectric layers consist of microbolometer structure for wavelength selectivity. All simulations are performed under the assumption that the sheet resistance of bolometer is 377 ohm. The relative dielectric constants of silicon nitride and silicon oxide are assumed to be 7.5 and 4, respectively. Also, it is assumed that a perfect mirror is located behind the bolometer layer. In the case of device 1, the total combinational thickness of 0.63 micron is comparable to "effective air thickness" of 1.445 micron.

For the range of wavelengths from 1 μm to 15 μm , the first resonance is generated at 5.78 μm . The second and third resonance are located at 1.93 μm and 1.12 μm , respectively. As shown in Fig. 3.5, there is tendency for the first resonance to be the widest and the third resonance is smaller than that of the second resonance in terms of wavelength resolution.

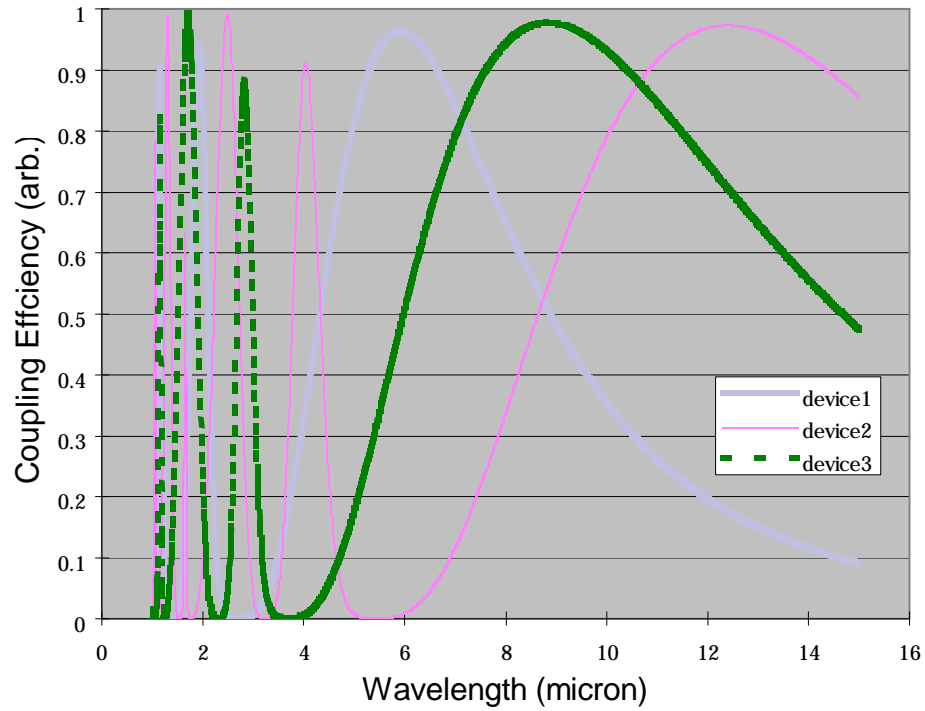


Figure 3.6 Simulation of the spectral response on multi stack micromachined structure with several air gaps.

	Si ₃ N ₄	SiO ₂	Si ₃ N ₄	Air cavity	Si ₃ N ₄	SiO ₂	Si ₃ N ₄
Device 1	707	5020	905	0	0	0	0
Device 2	750	4000	750	5000	750	4000	750
Device 3	400	2800	400	5000	400	2800	400

Table 3.1 The combination of dielectric layers that comprises the microbolometer structure for wavelength selection. The unit of thickness for each layer is Å.

Compared with device 1, the first resonance of device 2 and 3 is at longer wavelength location than that of device 1. That means that the first resonance of resonant air cavity microbolometer shown in device 2 and 3 cannot be lowered due to the limitation of total minimum thickness of the structure for mechanical stability, which is the minimum thickness of 5000 Å and is the thickness ratio of 3 and 3.5.

Figure 3.7 represents the result of the coupling efficiency in the frequency domain. Unlike wavelength representation, the location of each resonance point is equally spaced and the width at peak resonance is equal. Without a perfect reflecting mirror layer, device 1 shows a weak wavelength dependency because of interference effect due to the dielectric layers.

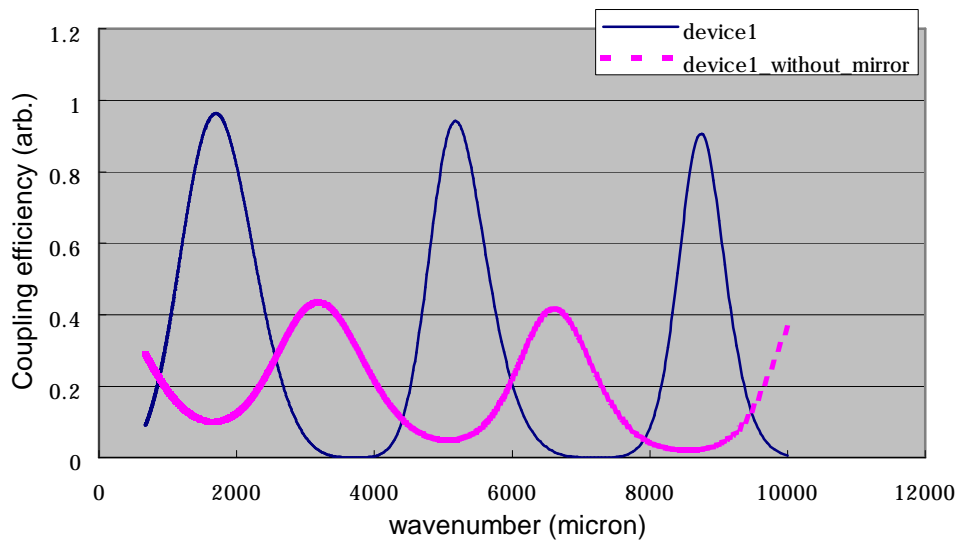


Figure 3.7 The frequency domain representation of spectral response of absorbed power coupling efficiency on specified device 1.

3.2.1 Effect of parameter variation

The parameters affecting the performance of an infrared detector can be investigated through simulation. The thickness variation of each dielectric layer can affect the resonance position of the incoming infrared signal. Under the assumption that process controllable thickness resides within 5% of the targeted process, the result of spectral absorbance is found in Figure 3.7. The important simulation results are summarized in table 3.2. For this calculation, other parameters such as sheet resistance and relative dielectric constant remain the same. The simulation is performed on a microbolometer with the thickness of 707 Å of silicon nitride, 5020 Å of silicon oxide, and 905 Å of silicon nitride. And then another simulation is applied to $\pm 5\%$ variation on the specified thickness of each layer. The 5% error in the thickness caused first resonance to shift in the amount of 0.29 μm , and the second and third resonance to shift as much as 0.1 μm and 0.02 μm , respectively.

Variation of the dielectric constant of each layer can be accounted for through effective thickness fluctuation. This variation may be influenced by process method and conditions. Variation of relative dielectric constant changes the effective air thickness as shown in equation (3.8). However, comparing with the effective thickness of 1.445 μm of device 1, 5% variation of relative dielectric constant resulted in the effective thickness of 1.409 μm as compared to 1.373 μm that is caused by 5% variation of actual thickness. That means that 5% thickness variation is a more dominant factor determining the shift in the resonance point.

The ideal sheet resistance of the microbolometer layer to establish the impedance matching is 377 ohm as shown before. If the sheet resistance of the bolometer mismatches the air impedance, coupling efficiency will be decreased without variation of each resonance point. Particularly, the width of first resonance will widen as sheet resistance is reduced. The relationship between sheet resistance and peak absorption is as shown in figure 3.10. As the sheet resistance varies farther from air impedance, the peak value of absorbed power decreases in the second and third resonance points.

Considering the bulk resistivity of the conductor, it is hard to achieve the sheet resistance of 377 ohm even with a couple of hundred-angstrom thickness. However, the resistivity of a thin conductor is very different from that of a bulk conductor. For example, the sheet resistance of chromium can be in the range of 50 – 330 ohm/sqr. This value is higher than sheet resistance calculated from bulk resistivity of chromium by factor of 5 [10][11].

In conclusion, the result of the simulation indicates that thickness variation causes the peak resonance to shift, and the mismatch of bolometer sheet resistance changes the amount of absorption of the incoming wave. The selectivity for specific wavelength is a little broad, and it may be required to have a band pass filter to enhance the sharpness of wavelength selectivity for the application.

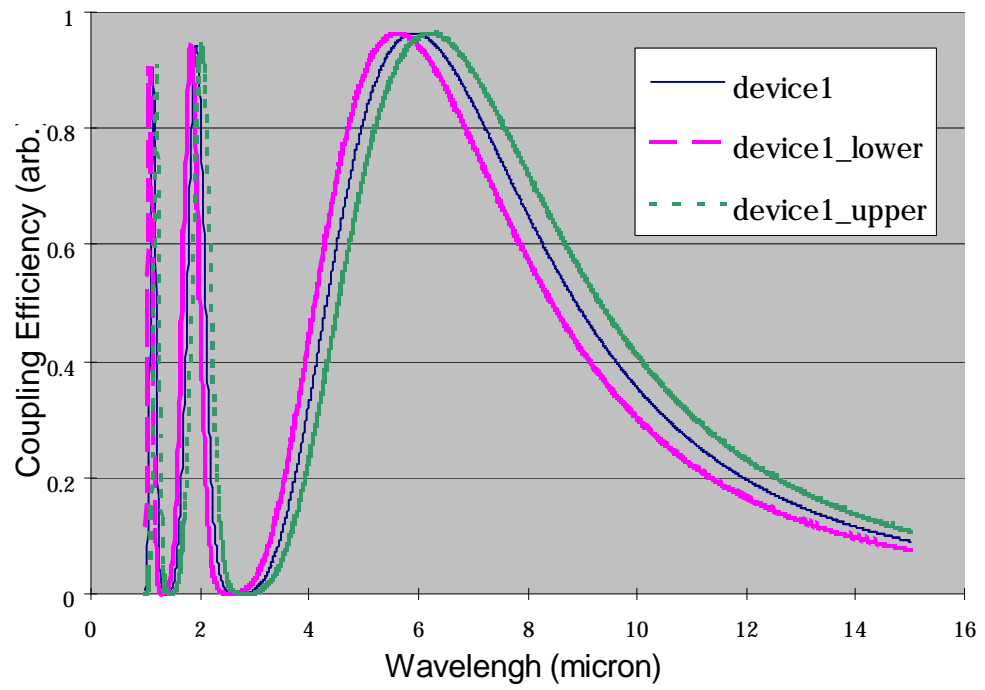


Figure 3.8 Effect of thickness variation on coupling efficiency of the incoming infrared signal.

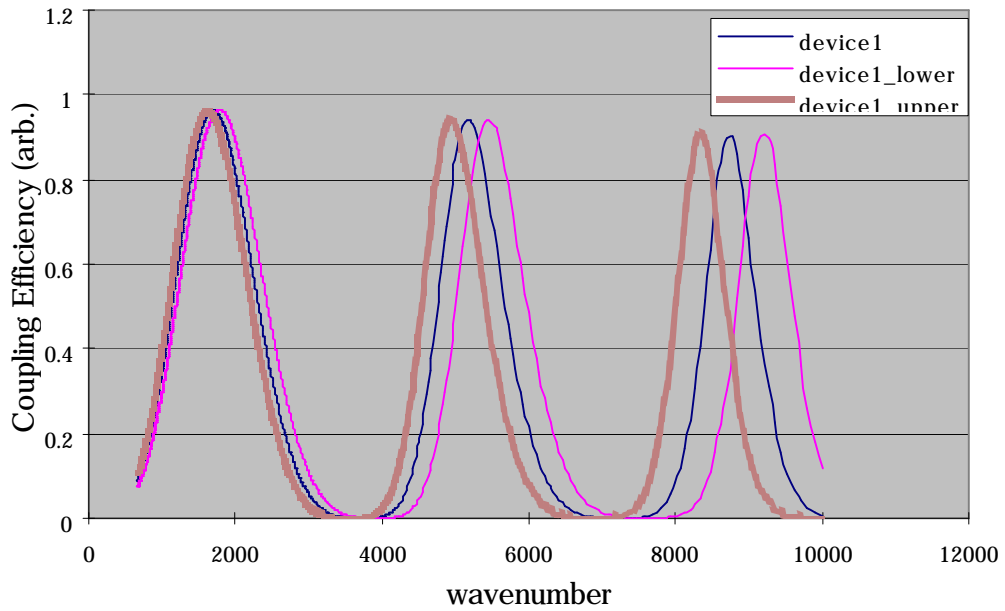


Figure 3.9 Effect of thickness variation on coupling efficiency of incoming infrared signal in frequency domain on device 1.

Actual thickness ($\text{Si}_3\text{N}_4 + \text{SiO}_2 + \text{Si}_3\text{N}_4$)	Effective air thickness	First resonance	Second resonance	Third Resonance
0.663 (device1)	1.445	5.78	1.93	1.12
0.630 (lower)	1.373	5.49	1.83	1.10
0.696 (upper)	1.518	6.07	2.02	1.21

Table 3.2. Summary of simulation on microbolometers with the thickness of 707 Å of silicon nitride, 5020 Å of silicon oxide, and 905 Å of silicon nitride with thickness variation of 5%. All units are in μm .

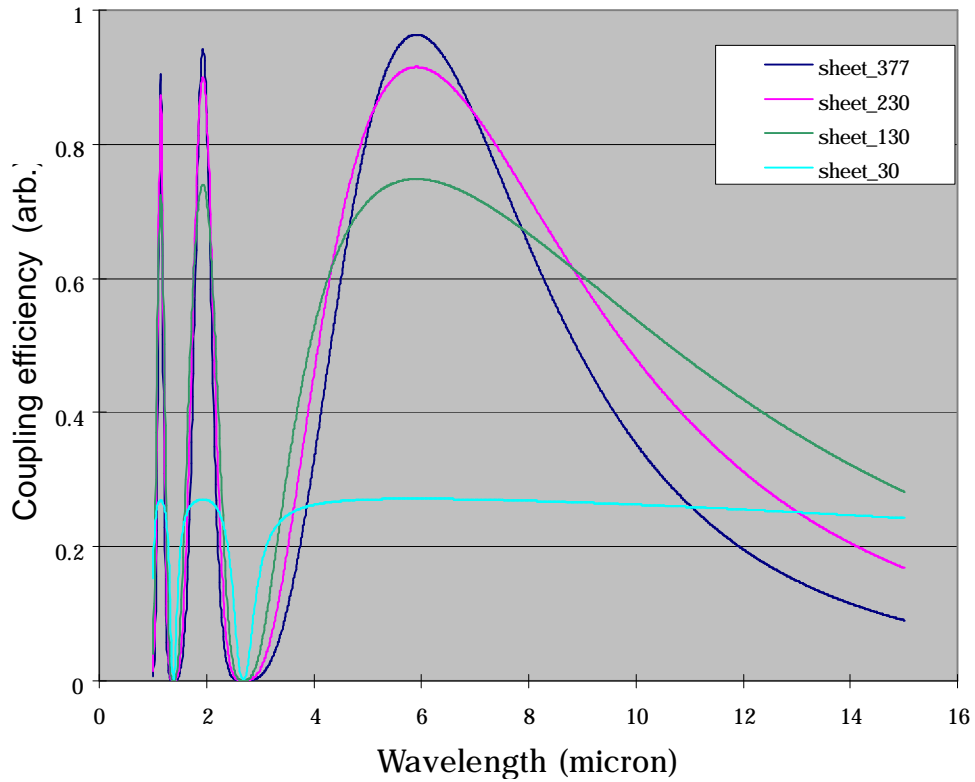


Figure 3.10 Effects on change of bolometer sheet resistance for coupling efficiency.

3.3 Resolving multi-wavelength ambiguities

By using the calculated absorbed power (P_{incident} times coupling efficiency) into equation (2.3), a detector signal output can be obtained.

$$V = I_b \cdot \frac{dR}{dT} \cdot \Delta T = I_b \cdot \frac{dR}{dT} \cdot P_{\text{absorbed}} \cdot Z_{\text{thermal}} \quad (2.3)$$

For a given effective air gap, response occurs at all wavelengths where $\lambda = 4 \cdot \text{gap} / (\text{odd integer})$. For a broadband incoming signal, a single detector cannot uniquely identify the wavelength of the incoming signal due to the multi spectral response.

To resolve multi wavelength ambiguities, a four “color” detector array configurations could be used [12]. In the following example it is assumed that an external band pass filter from just less than 2 μm to just over 10 μm is used.

Figure 3.11 illustrates the possible solution for resolving the multi-wavelength ambiguities. For an equivalent air gap of 2.5 μm , the response occurs at 10 μm , 3.3 μm , and 2 μm within the operating wavelength region. The detector having a 1.5 μm gap can be built to produce the resonance at 2 μm and shorter. Finally, by the fabrication of device with a 0.5 μm and 0.83 μm gap, the signal output at 2.5 μm air gap device can be achieved by subtracting the response of 0.5 μm and 0.83 μm gap device. If the detector has a 0.83 μm air gap, the response of spectral resonance occurs at 3.3 μm . It enables to extract the signal output at 1.5 μm air gap device by subtracting the response of 0.5 μm gap device. Using the relationship described in equation (3.9) and (3.10), the response at specific wavelength from broadband source can be resolved.

$$S_{10} = S_{\text{gap}_{2.5}} - m_{3.3 \rightarrow 10} \cdot S_{\text{gap}_{0.83}} - m_{2 \rightarrow 10} \cdot S_{\text{gap}_{0.5}}, \quad (3.9)$$

$$S_6 = S_{\text{gap}_{1.5}} - m_{2 \rightarrow 6} \cdot S_{\text{gap}_{0.83}} - m_{2 \rightarrow 10} \cdot S_{\text{gap}_{0.5}}, \quad (3.10)$$

where S_{10} and S_6 are the response signal at 10 μm and 6 μm respectively, $S_{\text{gap}_{2.5}}$ is the response of 2.5 μm gap detector, S_{gap_n} is the response of n μm gap detector, $m_{3.3 \rightarrow 10}$ is the fitting parameter of coupling from response signal at 3.3 μm to response signal at 10 μm , and $m_{2 \rightarrow 10}$ is the fitting parameter of coupling from response signal at 2 μm to response signal at 10 μm

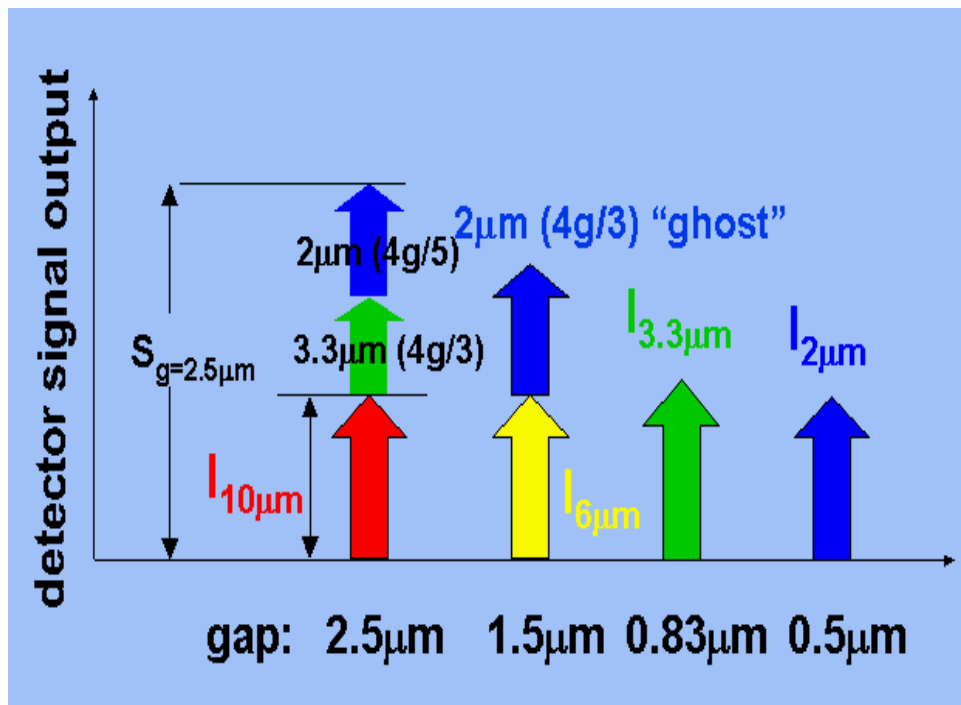


Figure 3.11 Resolving multi-wavelength ambiguities using 4 color detector arrays.

3.4 Summary

In this chapter, a method of impedance matching for a thin conductor absorber is introduced. To achieve the wavelength selectivity, microbolometer structure is configured by placing the perfect mirror at $[(\text{odd integer})/4] * \lambda$ behind the absorbing layer. To interpret the absorbed power coupling efficiency, a transmission line equivalent circuit model associated with physical structure is explained. Finally, the result of simulation using a model is calculated on different structures, and a possible method of resolving multi-wavelength ambiguities is suggested.